# Dual-Band Active Integrated Antenna with Electronically Controllable for S-Band Applications

**Jasem Jamali [1], Masoud Ahmadi [2], Jalil Mazloum [3], Mohammad Ojaroudi [4]**

[1] Department of Electrical Engineering
Kazerun Branch, Islamic Azad University, Kazerun, Iran

[2] Faculty of Electrical & Computer Engineering
Shahid Beheshti University, Tehran, Iran

[3] Faculty of Electrical Engineering
Shahid Sattari Aeronautical University of Science and Technology, Tehran, Iran

[4] Young Researchers and Elite Club, Ardabil Branch
Islamic Azad University, Ardabil, Iran
m.ojaroudi@iauardabil.ac.ir

***Abstract*** ─ A novel reconfigurable active feedback antenna for WiMAX/WLAN applications is presented. By using an H-shaped radiating patch with a pair of C-shaped slots in the active feedback antenna, two new resonances can be achieved. Also, the proposed radiating patch has a major advantage in providing tighter capacitive coupling to the line in comparison to known radiating patch. In order to generate DC isolation in the RF path, we use a pair of gap distances in the microstrip loop. Also, by using the [S] parameters of the active element, a novel design of the microwave oscillator is performed. Simulated and experimental results obtained for this antenna show that the proposed Active Integrated Antenna (AIA) has a good return loss and radiation behavior within the WiMAX/WLAN frequency range.

***Index Terms*** ─ C-shaped slot, H-shaped radiating patch, Reconfigurable Active Integrated Antenna (RAIA), WiMAX/WLAN systems.

## I. INTRODUCTION

In the last few years, there have been rapid developments in various antenna designs for wireless local area network (WLAN) and worldwide interoperability for microwave access (WiMAX) applications. These antennas include the planar inverted-F antennas (PIFAs) [1], printed patch antenna [2], the CPW-fed antennas [3], and the planar monopole antennas [4]. However, up to now, a printed antenna that has T-shaped notch configuration has not been reported.

It is a well-known fact that, active feedback presents really appealing physical features, such as simple structure, small size, and low cost. Because of all these interesting characteristics, multi-band low noise amplifier is expected to become a key device for the next generation of multi-band and multi-mode wireless radios [5], and growing research activity is being focused on them [6-8]. Various switching based techniques have been proposed to achieve multi-band performance. Some of the topologies use separate oscillators [5] to obtain multi-band response, while others use distinct resonators [6] or matching networks [7] to achieve the same.

In this paper, we propose a novel frequency reconfigurable active integrated antenna with the capability to switch between WLAN and WiMAX modes. The antenna which uses a switchable slotted structure for reconfigurability, has a simple structure and smallest size in comparison to antennas reported in literature [1]-[4]. In the proposed structure, based on electromagnetic coupling (EC), an H-shaped radiating patch with a

*Submitted On: April 14, 2013*
*Accepted On: September 5, 2014*

pair of C-shaped slots in the active feedback antenna is used to perturb two resonance frequencies at 2.4 GHZ (WLAN) and 3.5 GHz (WiMAX). This structure has a major advantage in providing tighter capacitive coupling to the line in comparison to known radiating patch [9]. The proposed antenna has three different switchable states: 2.25-10.72 GHz in WLAN mode, 3.34-3.71 GHz in WiMAX mode, and 1.65-1.89 GHz in narrowband mode. Also, the implemented dual-band low noise amplifier exhibited output power level of 12.84 dB at frequency of 2.4 GHz and 10.94 dB at frequency of 3.49 GHz, for various diodes bias conditions.

## II. RECONFIGURABLE ANTENNA DESIGN

The proposed passive antenna fed by a 50-Ω feed line is shown in Fig. 1, which is printed on a FR4 substrate of thickness 0.8 mm and permittivity 4.4. The numerical and experimental results of the input impedance and radiation characteristics are presented and discussed. The Ansoft simulation software high-frequency structure simulator (HFSS) [10] is used to optimize the design and agreement between the simulation and measurement is obtained.

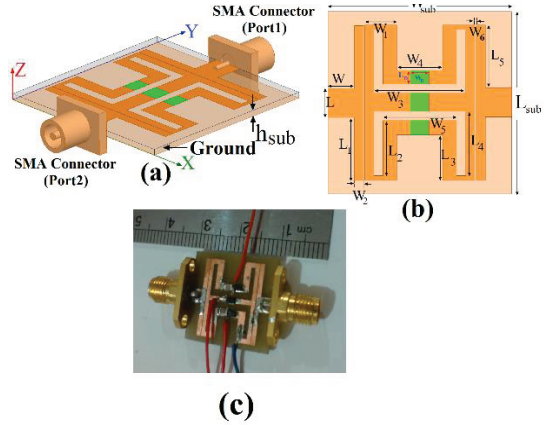


Fig. 1. Configuration of the switchable antenna: (a) side view, (b) top view, and (c) fabricated scheme.

To design a novel reconfigurable antenna, three pin diodes are inserted in the radiating patch of the proposed antenna as displayed in Fig. 1. Three states with different conditions of diodes are specified in Table 1 as states 1, 2 and 3. Figure 2 shows simulated and measured return loss characteristics for the proposed antenna in three states 1, 2, and 3 with pin diodes as depicted in Table 1. As depicted in Fig. 2, in this structure, the H-shaped radiating patch with a pair of C-shaped slots with three p-i-n diodes is used in order to electronically switch between the WLAN (2.4 GHz) and WiMAX (3.45 GHz) frequency bands. Also, when the central diode is biased and the others are off, the proposed antenna has not any radiation performance in the S-band. In addition, this structure has a major advantage in providing tighter capacitive coupling to the line in comparison to known radiating patch [2]. In the proposed configuration, a pair of gap distances are playing an important role in the radiating characteristics of this antenna, because it can adjust the electromagnetic coupling effects between the H-shaped radiating patch and the microstrip transmission line [4].

Table 1: Three states of proposed antenna with different conditions for pin diodes

| State | D1 | D2 | D3 |
|---|---|---|---|
| 1 | On | Off | On |
| 2 | On | On | On |
| 3 | Off | On | Off |

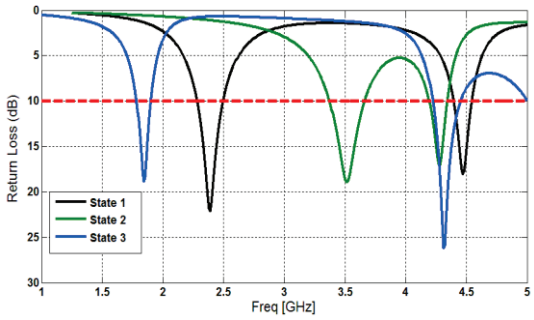


Fig. 2. Simulated return loss characteristics for the passive microstrip antenna with various states of diodes.

The optimal dimensions of the designed passive antenna are as follows: $W_{sub}$=20 mm, $L_{sub}$=20 mm, $h_{sub}$=0:8 mm, W=4 mm, L=1.5 mm, $W_1$=3 mm, $L_1$=7 mm, $L_2$=4 mm, $W_2$=0.85 mm, $L_3$=3 mm, $W_3$=8 mm, $L_4$=4 mm, $W_4$=4 mm, $L_5$=7 mm, $W_5$=6 mm, $W_6$=0.15 mm, $W_P$=2 mm, and $L_P$=1 mm.

For applying the DC voltage to PIN diodes, metal strips with dimensions of 2 mm × 0.6 mm were used inside the main slot. Moreover, for each PIN diode a 100 pF DC blocking capacitor was placed in the slot to create the RF connection of the

PIN diode and also to isolate the RF signal from the DC. In the introduced design, HPND-4005 beam lead PIN diodes [11] with extremely low capacitance were used. For biasing PIN diodes a 0.7 volts supply is applied to metal strips. The PIN diodes exhibit an ohmic resistance of 4.6 Ω and capacitance of 0.017 pF in the on and off states, respectively. By turning diodes on, the metal strips are connected to the ground plane and become a part of it. Therefore, a part of the slot is short-circuited, and the corresponding resonance is eliminated due to the change in main slot's length. The desired frequency band can be selected by varying the states of PIN diodes which changes the total equivalent length of the slot.

In order to understand the phenomenon behind switching electronically between WLAN and WiMAX resonance frequency, the simulated current distributions on the radiating patch of the proposed antenna for on and off statuses of the p-i-n diodes, are presented in Figs. 3 (a), (b) and (c), respectively. As shown in Fig. 3 (a), at the WLAN resonance frequency (2.4 GHz) the current mainly concentrates on the C-shaped strips edges, and also it can be seen that the electrical current does change its direction along these strips. In addition, the current mainly concentrates on the central strip at the WiMAX resonance frequency (3.5 GHz), as shown in Fig. 3 (b).

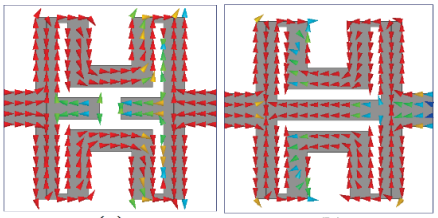


Fig. 3. Simulated surface current distributions on the radiating patch for the proposed antenna shown in Fig. 1: (a) state 1 at 2.4 GHz, and (b) state 2 at 3.5 GHz.

## III. RECONFIGURABLE LOW NOISE APMLIFIER DESIGN

Transistor low noise amplifier can be designed using either bipolar or GaAs MESFET devices [12-13]. In order that the amplifier delivers a maximum power to the load, it must be properly terminated at output port to a resistor [14-15]; hence, the need of an input/output matching circuit arises. A short and efficient CAD procedure for the design of reconfigurable dual-band microstrip amplifier is performed. It is based on the scattering-matrix parameters of the active element. The CAD procedure has mainly two steps. The first step is the design of a narrowband high-gain amplifier operating at the first frequency of 2.4 GHz, and the developed full-scale simulation program is used for stability consideration and analytical design of the input and output matching circuits [13]. The second step is to design lengths and widths of the second input and output matching circuits so as to get a narrowband high-gain amplifier operating at the second frequency of 3.5 GHz. Using the [S] parameters of the active element, the design of the microwave amplifier is performed using our full-scale computer simulation program. First, the stability of device can be checked by two stability factors K and |Δ|. The mathematical equations for K and |Δ| are [14]:

$$\Delta = S_{11}S_{22} - S_{21}S_{12}, \tag{1}$$

$$K = \frac{1-|S_{11}|^2-|S_{22}|^2+|\Delta|^2}{2|S_{21}S_{12}|}. \tag{2}$$

The stability of the used ATF 13786 GaAs transistor at the frequencies of 2.4 GHz and 3.5 GHz is calculated through calculation of the stability factor, K and Δ [15]. The transistor is potentially unstable at the operated frequencies 2.4 GHz and 3.5 GHz (i.e., K=0.5718 and K=0.656, respectively).

The matching networks are designed to get minimum reflection coefficient at the transistor input and output. The analytical design of the terminating circuit and the output matching circuit are performed using the developed computer program [14]. In this design, the input and output matching circuits are designed to transfer the calculated $Z_{MS}$* and $Z_{ML}$* to 50 Ω. The input and output matching circuits can be designed using two-section matching circuits (a series transmission line and an open/short single/balanced shunt stub). The analytical design procedure of the matching circuits is as follows:

$$\Gamma_{MS} = \frac{B_1 - \sqrt{B_1^2 - 4C_1^2}}{2C_1}, \tag{3}$$

$$\Gamma_{ML} = \frac{B_2 - \sqrt{B_2^2 - 4C_2^2}}{2C_2}, \tag{4}$$

$$B_1 = 1 + |S_{11}|^2 - |S_{22}|^2 - |\Delta|^2, \tag{5}$$

$$B_2 = 1 + |S_{22}|^2 - |S_{11}|^2 - |\Delta|^2, \quad (6)$$

$$C_1 = S_{11} - conj(S_{22}).\Delta, \quad (7)$$

$$C_2 = S_{22} - conj(S_{11}).\Delta, \quad (8)$$

$$G_{T\max} = \frac{1}{1-|\Gamma_S|^2}|S_{21}|^2 \frac{1-|\Gamma_L|^2}{|1-S_{22}\Gamma_L|^2}, \quad (9)$$

$$Z_{in} = Z_0 \frac{1-|\Gamma_S|^2 + 2j|\Gamma_S|\sin(\theta_{\Gamma_S})}{1+|\Gamma_S|^2 - 2|\Gamma_S|\cos(\theta_{\Gamma_S})}, \quad (10)$$

$$Z_{Out} = Z_0 \frac{1-|\Gamma_L|^2 + 2j|\Gamma_L|\sin(\theta_{\Gamma_L})}{1+|\Gamma_L|^2 - 2|\Gamma_L|\cos(\theta_{\Gamma_L})}, \quad (11)$$

$$Y_{in} = \frac{1}{Z_{in}}, \quad (12)$$

$$Z_{o1} = \frac{1}{|imag(Y_{in})|}, \quad (13)$$

$$Z_{o2} = \sqrt{\frac{Z_0}{|\mathrm{Re}(Y_{in})|}}, \quad (14)$$

$$Y_{Out} = \frac{1}{Z_{out}}, \quad (15)$$

$$Z_{o3} = \frac{1}{|imag(Y_{Out})|}, \quad (16)$$

$$Z_{o4} = \sqrt{\frac{Z_0}{|\mathrm{Re}(Y_{Out})|}}. \quad (17)$$

A prototype reconfigurable LNA circuit was designed on a FR4 substrate with 0.8 mm thickness for wireless applications. Microstrip lines were used for the input and output matching network, rather than utilizing lumped elements to minimize overall insertion losses. By tuning the length of the microstrip lines, the circuits operate at a different frequency. A schematic diagram of the reconfigurable LNA design is shown in Fig. 4 with the lumped elements, such as capacitors and resistors and the transistor's position. Figure 5 shows hard-wire connected reconfigurable LNA configured at 2.4 GHz which can also be reconfigured to operate at 3.5 GHz. Amplifier biasing circuit passive part is fabricated with available microstrip materials (FR4) using wet etching technique, active part is soldered on the passive substrate. The input and output ports are matched to 50-ohm transmission line, which is a microstrip line with 1.5 mm width. Some pads should be grounded and therefore there are some connections to the reference ground plane using via that is shown in the layout with dark gray circles. The conductive connections inside these holes are made by punching some metallic bars in the holes and soldering them to each face of the board.

Simulated S-parameters results for the proposed LNA for WLAN application at 2.4 GHz, and WiMAX applications at 3.5 GHz are shown in Fig. 6 and Fig. 7, respectively. All design steps for matching networks, stability, and DC biasing were done using schematic wizard of Advanced Design System (ADS) by Agilent Technologies [18] using the model provided by CEL for that transistor.

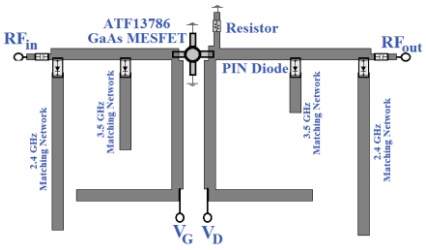


Fig. 4. Reconfigurable LNA concept diagram with two various matching stubs to operate at 2.4GHz and 3.5 GHz.

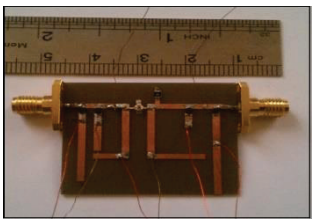

Fig. 5. Fabricated reconfigurable LNA configured at 2.4 GHz which can also be reconfigured to operate at 3.5 GHz.

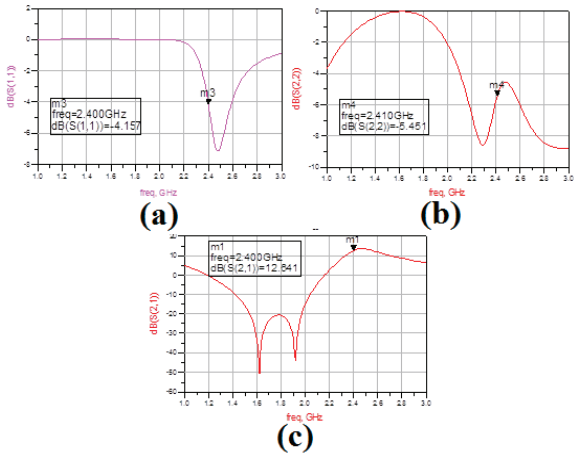


Fig. 6. Simulated results for the proposed LNA for WLAN application at 2.4 GHz: (a) $S_{11}$, (b) $S_{22}$, and (c) $S_{21}$.

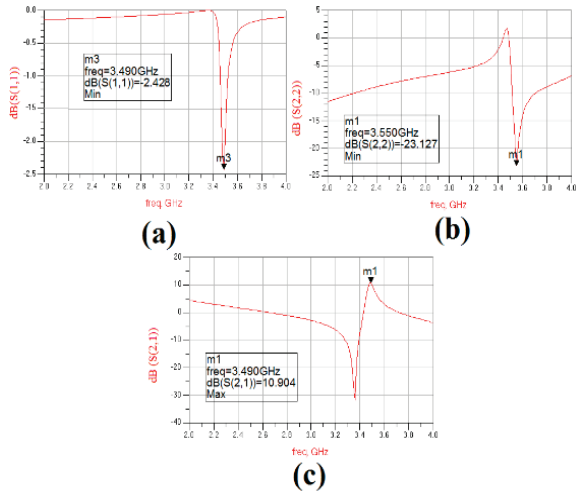


Fig. 7. Simulated results for the proposed LNA for WiMAX application at 3.5 GHz: (a) $S_{11}$, (b) $S_{22}$, and (c) $S_{21}$.

## IV. RECONFIGURABLE ACTIVE INTEGARTED ANTENNA

The presented active feedback antenna is shown in Fig. 8, which is printed on an FR4 substrate of thickness 0.8 mm, permittivity 4.4, and loss tangent 0.018. The proposed active feedback antenna structure consists of a rectangular ring with a pair of protruded Γ-shaped strips for radiating element, a microstrip loop, and an oscillator with DC bias circuit and matching circuit for active part. The width of the 50-Ω microstrip line is fixed at 1.5 mm, as shown in Fig. 6. The matching circuit to the left and right of the device controls the coefficient of feedback. On the other side of the substrate, a conducting ground plane is placed. In addition, to satisfy the oscillation-phase requirement, the microstrip loop is fixed to a suitable electrical length, taking the calculated phases of the oscillator and passive antenna into consideration [16].

Figure 9 shows the measured return loss characteristics for the active antenna in comparison of simulated return loss characteristics for the passive microstrip antenna with various states of diodes. The fabricated antenna satisfies the 10-dB return loss requirement within the WiMAX/WLAN frequency range. However, as shown in Fig. 9, there exist a discrepancy between measured data and the simulated results. This discrepancy is mostly due to a number of parameters, such as the fabricated antenna dimensions as well as the thickness and dielectric constant of the substrate on which the antenna is fabricated, the wide range of simulation frequencies and also the effect of pin diode and its biasing circuit.

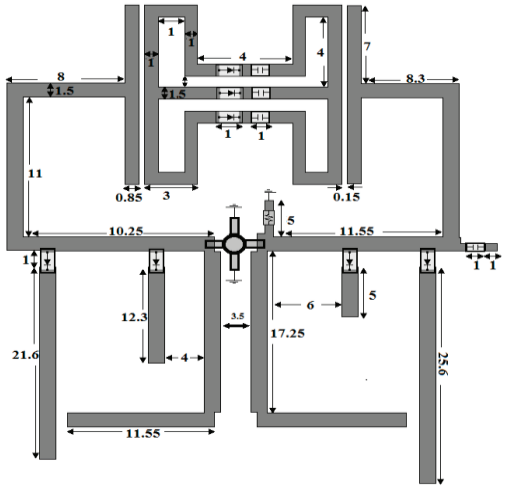


Fig. 8. Configuration of the proposed active integrated antenna (unit: mm).

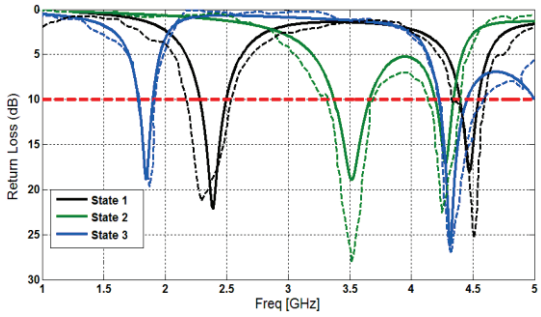


Fig. 9. Measured return loss characteristics for the active antenna in comparison of simulated return loss characteristics for the passive microstrip antenna with various states of diodes (dashed line: measured, solid line: simulated).

The simulated radiation patterns including the co-polarization and cross-polarization for the E-plane (y-z plane) and H-plane (x-z plane) at the resonance frequencies are shown in Fig. 10. The simulated radiation patterns are calculated by using the gap-source technique with the commercial EM simulator HFSS, considering the complete active feedback antenna which has same layout, except with an active transistor [3]. The received cross-polarizations in the E-plane and H-plane of the AIA are approximately 17 and 14 dB lower than the maximum co-polarized radiation, respectively. As

seen in Fig. 10, the radiation pattern in the H-plane is asymmetrical, due to the asymmetrical presence of the distributed oscillator-feedback circuitry. The designed feedback-antenna oscillator has stable oscillation. The obtained gain by the amplifier is of 11.2 dB.

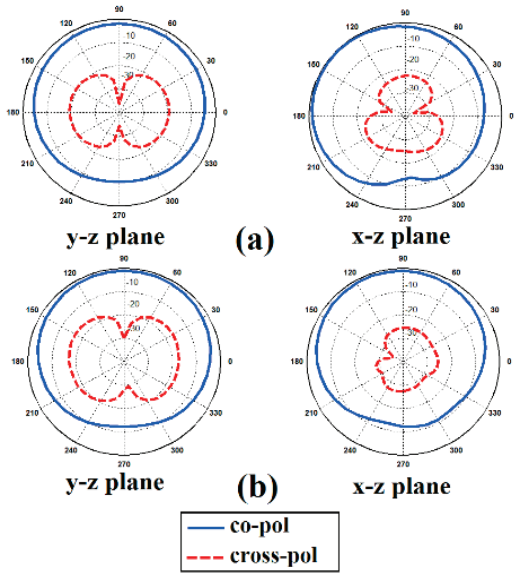


Fig. 10. Simulated radiation patterns of the proposed active integrated antenna.

## V. CONCLUSION

As presented above, a novel design of reconfigurable active integrated antenna with electronically controllable is an interesting subject for for WiMAX/WLAN applications. By using an H-shaped radiating patch with a pair of C-shaped slots in the active feedback antenna, two new resonances can be achieved. The proposed antenna has three different switchable states: 2.25-2.72 GHz in WLAN mode, 3.34-3.71 GHz in WiMAX mode, and 1.65-1.89 GHz in narrowband mode. The LNA design based on the AIA concept has been shown to provide an efficient and successful method for designing high efficiency and compact systems. The implemented dual-band low noise amplifier exhibited output power level of 12.84 dB at frequency of 2.4 GHz and 10.94 dB at frequency of 3.49 GHz, for various diodes bias conditions.

## REFERENCES

[1] F. R. Hsiao and K. L. Wong, "Compact planar inverted-F patch antenna for triple-frequency operation," *Microwave Opt. Technol. Lett*., 33, 459-462, 2002.

[2] J. Lu and H. Chin, "Planar compact U-shaped patch antenna with high-gain operation for Wi-Fi/WiMAX application," *Applied Computational Electromagnetics Society (ACES) Journal*, vol. 26, no. 1, pp. 82-86, January 2011.

[3] S. Bashiri, C. Ghobadi, J. Nourinia, and M. Ojaroudi, "CPW-fed slot-like sleeve monopole antenna with bandwidth enhancement for UWB wireless communications," *ACES Journal*, vol. 28, no. 9, pp. 815-820, 2013.

[4] M. Ojaroudi and E. Mehrshahi, "High accuracy time domain modeling of microstrip discontinuities by using modified TDR based on barker codes with flat spectrum and integrated side-lobes," *ACES Journal*, vol. 28, no. 5, pp. 374-379, May 2013.

[5] K. Chang, "Active integrated antennas," *Proc. IEEE*, vol. 50, no. 3, March 2002.

[6] P. S. Hall, P. Gardner, and G. Ma, "Active integrated antenna," *IEICE Trans. Commun*., E85-B, (9), pp. 1661-1666, 2002.

[7] M. Ojaroudi and N. Ojaroudi, "Ultra-wideband small rectangular slot antenna with variable band-stop function," *IEEE Transactions on Antenna and Propagation*, vol. 62, no. 1, pp. 490-494, January 2014.

[8] G. Yun, "Compact oscillator-type active antenna for UHF RFID reader," *Electronic Letters*, vol. 43, no. 6, March 2007.

[9] A. Faraghi, M. N. Azarmanesh, and M. Ojaroudi, "Small microstrip low-pass filter by using novel defected ground structure for UWB applications," *Applied Computational Electromagnetics Society (ACES) Journal*, vol. 28, no. 4, pp. 341-347, April 2013.

[10] Ansoft High Frequency Structure Simulation (HFSS), ver. 13, Ansoft Corporation, 2010.

[11] HPND-4005, "Beam lead PIN diode," Avago Technologies.

[12] K. Chang, "Active integrated antennas," *Proc. IEEE*, vol. 50, no. 3, March 2002.

[13] P. S. Hall, P. Gardner, and G. Ma, "Active integrated antenna," *IEICE Trans. Commun*., E85-B, (9), pp. 1661-1666, 2002.

[14] M. Ojaroudi and E. Mehrshahi, "Bandwidth enhancement of small square monopole antennas by using defected structures based on time domain reflectometry analysis for UWB applications," *ACES Journal*, vol. 28, no. 7, pp. 620-627, July 2013.

[15] E. M. Biebl, "Millimeter wave systems based on active integrated antennas," *Antennas and Propagation Millenium Conference, European Space Agency*, Davos, 2000.